The luminescence efficiency of green phosphor Ca$_7$(PO$_4$)$_2$(SiO$_4$)$_2$:Eu^{2+} for white light-emitting diode

Van Liem Bui[1], Phan Xuan Le[2]

[1]Faculty of Fundamental Science, Industrial University of Ho Chi Minh City, Ho Chi Minh City, Vietnam
[2]Faculty of Mechanical-Electrical and Computer Engineering, School of Engineering and Technology,
Van Lang University, Ho Chi Minh City, Vietnam

Article Info

ABSTRACT

This study examines the green-emission phosphor composition of Eu^{2+} doped Ca$_7$(PO$_4$)$_2$(SiO$_4$)$_2$ to serve the goal of efficiency enhancement for the white light emitting diode (LED). The process of preparation and photoluminescent investigation of proposed phosphor composition was monitored under near UV excitation wavelength of the LED die. The sample phase was determined using X-ray diffractometer (XRD). To explore Ca$_7$(PO$_4$)$_2$(SiO$_4$)$_2$:Eu^{2+} capabilities, the diffuse reflectance and photolumine-scence spectral figures were employed. The ultraviolet absorption of Ca$_7$(PO$_4$)$_2$(SiO$_4$)$_2$:Eu^{2+} ranged from 240 to 440 nm, with a wide band of green emission peaking at 522 nm. Besides the concentration quenching mechanism, we also focus on essential characteristics for white-light-emitting diode (WLED) production like temperature-dependent lumen output and chromaticity coordinates.

Corresponding Author:

Phan Xuan Le
Faculty of Mechanical-Electrical and Computer Engineering, School of Engineering and Technology
Van Lang University
Ho Chi Minh City, Vietnam
Email: le.px@vlu.edu.vn

1. INTRODUCTION

The remarkable brightness, long-time use, and power efficiency are the critical features that make the white-light- emitting diode (WLED) using down-conversion phosphors stand out in the new lighting industry and marke [1], [2]. From the very early production, the parts of a WLED package included an InGaN-based blue chip [3]–[6] and a yellow phosphor Y$_3$Al$_5$O$_{12}$:Ce^{3+} (YAG:Ce). This combination gave out high luminescence output, however, owing to the absence of the components with red color, a fairly poor hue rendering indicator (CRI) and elevated hue temperature were its significant limitations. CRI values of the common phosphor-conversion WLED with high luminous performance was below 80 for correlate color temperature (CCT) less than 6,000 K, compared to 100 for incandescent and 82-85 for fluorescent lights [7]. Phosphors having red illumination that can be effectively stimulated by blue illumination are needed to solve this problem, and these phosphors commonly are nitrides [8]. Almost all nitride-type phosphors, on the other hand, necessitate costly raw materials and the high-temperature with high-pressure preparation procedure, thus may require more stages and consume more time in fabrication. When there was the increasing electrical currents, the color shifts of WLEDs from white to blue owing to the heat quenching characteristic of the the yellow YAG:Ce phosphor particles, allowing the control of more blue rays from the light emitting diode (LED) chip to occur. Because ultraviolet (UV) light is invisible, the growth of an UV LED chip with AlGaN base [9]–[11] coupled with red-green-blue (RGB) phosphors, which means red, green, and blue phosphors,

could eliminate the foregoing problems. In recent years, there has been a lot of research on the pairing of UV LED chips with RGB phosphors. As a result, the luminescence qualities of the phosphors utilized have a dramatical impact on the final productivity of UV LEDs. Exploring novel RGB phosphors triggered by UV light therefore has been one of the interesting and practical study topics in the down-conversion phosphor aspect. Because of the outstanding performance in terms of either physical or chemical stability and affordable cost of production, rare-earth-doped silicate materials have been extensively inspected for usage in UV LEDs [12]–[14]. Materials with Eu^{2+} doped alkaline earth silicates have piqued researchers' curiosity. Eu^{2+} dopant can be easily distributed in the host matrix of an alkaline earth silicate to generate light. In β-$Ca_2SiO_4:Eu^{2+}$ (β-$C_2S:Eu^{2+}$), for instance, Eu^{2+} prefers to occupy Ca^{2+} sites and produces vivid green lights [12]. The isomers of β-Ca_2SiO_4 i.e., α′-Ca_2SiO_4 and α-Ca_2SiO_4, are unstable until the source material $Ca_3(PO_4)_2$ is added [15], [16]. The Eu^{2+} doped $Ca_{15}(PO_4)_2(SiO_4)_6$ ($C_{15}P_2S_6$), which is the stable phase of α′-Ca_2SiO_4, has recently been identified as a good candidate for UV LEDs [16]. Li *et al.* [17] identified Nagelschmidtite [$Ca_7(PO_4)_2(SiO_4)_2(C_7P_2S_2)$] as the stable phase of α-Ca_2SiO_4, which is ascribed to the substituting process of one of the SiO_4 tetrahedra and Ca sites of α′-Ca_2SiO_4 by PO_4 tetrahedron and Ca vacancy (V), in turn, relying on the reaction: 2 SiO_4+Ca 2 PO_4+V. In light of the foregoing, $C_7P_2S_2$ could be a good host lattice for Eu^{2+}. According to Peng *et al.* [18], the $C_7P_2S_2:Eu^{2+}$ phosphorus composition with yellowish-green emission was produced using the sol-gel method. It might be difficult for the original synthesis approach of $C_7P_2S_2$ to be realized for extensive utilization in large-scale productions since the wet chemical synthesizing technique was included. Consequently, the $C_7P_2S_2:Eu^{2+}$ was produced using a solid-state process in this study. This work reports on the photoluminescence properties of $C_7P_2S_2:Eu^{2+}$ that separate it from those reported in the work of Peng *et al.* [18], and the prospective application of $C_7P_2S_2:Eu^{2+}$ in LEDs are experimentally detailed in this research.

2. EXPERIMENTAL DETAILS
2.1. Preparation of green phosphor $Ca_7(PO_4)_2(SiO_4)_2:Eu^{2+}$ ($C_7P_2S_2:Eu^{2+}$)
In this step, we use a solid-state reaction technique to create the phosphor $C_7P_2S_2:Eu^{2+}$ with strong green emission. $CaCO_3$ (99.5%), Eu_2O_3 (99.99%), $NH_4H_2PO_4$ (AR), and SiO_2 (AR) were the initial components. Then, using ethanol as a solvent to utterly combine the raw materials with $Ca_{7-x}Eu_x(PO_4)_2(SiO_4)_2$ (0.5% ≤x≤ 7%). The mixes were then burned for 6 hours at 1500 °C in an H_2/N_2 environment. Finally, the samples were pulverized with an agate mortar after being cooled down to normal temperature in the furnace [19].

The phase of the samples was collected and examined utilizing a X-ray diffractometer (XRD). Utilizing $BaSO_4$ as a standard reference, diffuse reflectance spectra were acquired using a UV-vis spectrophotometer. This stage uses the spectrofluorometer equipment to measure both excitation and emission spectra. The emission illumination and a conventional elevated heat fluorescence controller were used to perform the phosphor's temperature-dependent emitted luminescence spectra.

2.2. Characterization of phosphor
Except for the emission intensity, the form of all emission spectra does not change much as Eu^{2+} concentration rises. The brightness rises as the dopant concentration rises until it reaches 3%, then drops owing to concentration quenching. According to blasse [10], [20], [21], the critical transfer distance (R_c) can be determined by the distance at which the likelihood of energy transfer matches Eu^{2+} radioactive emission's probability, as indicated in (1).

$$Rc \approx 2\left(\frac{3V}{4\pi X_cN}\right)^{\frac{1}{3}} \tag{1}$$

Where V is the unit cell's volume, X_c is the activator ion's critical concentration, and N is the quantity of formula units per unit cell. In the instance of $C_7P_2S_2:Eu^{2+}$, we find the emission quenching when x>3%. When the X_c is 3%, R_c is estimated as 28.67 when V=8877.563 and N=24 are used. Because of the dominance of the exchange interaction at a small distance (normal critical distance is 5 Å [21]), the energy transfer in this scenario will be solely by electric multipolar interaction. There are types of multipole-multipole interactions, relying on Dexter's theory, including dipole-dipole (*d-d*), dipole-quadrupole (*d-q*), and quadrupole-quadrupole (*q-q*). Thus, the radiation strength (I) of the multipolar interaction may be defined using the shift emitting strength from the emitting level regarding multipolar interaction, whose computation is demonstrated in the following expression [20], [22], [23].

$$I/x = K\left[1 + \beta(x)^{\theta/3}\right]^{-1} \tag{2}$$

Where we show the radiation strength, x is the activator ion concentration, and K and β are constants under similar excitation circumstances. Thus, θ expresses the function of multipole-multipole interaction for 6 (*d-d*), 8 (*d-q*), or 10 (*d-q*). The dependence of lg(I/x) on lg(x) is plotted for the accurate result of the two emission centers, from which a straight line with a -θ/3 slope is obtained. Since the concentration quenching of Eu^{2+} in $C_7P_2S_2:Eu^{2+}$ were identified to be around 3%, I/x is a function of x ≥ 3%. When the relationship between lg(I/x) and lg(x) is linear with a 1.81 slope, θ is estimated to be around 6, indicating the *d-d* interaction is the concentration quenching mechanism of Eu^{2+} radiation in the $C_7P_2S_2:Eu^{2+}$.

The phosphor layer of an actual WLED is replicated with flat layer of silicone using the LightTools 9.0 application and the Monte Carlo approach. This simulation takes place through two different periods: i) it is very important to establish and create multi-chip white LED (MCW-LED) lamp configuration models and optical characteristics and ii) lighting impacts of $C_7P_2S_2:Eu^{2+}$ phosphor composition are followingly controlled by its concentration v arieties. We must establish several cont-rasts to determine the effect of $YAG:Ce^{3+}$ and $C_7P_2S_2:Eu^{2+}$ phosphor composition above the output of MCW-LED lights. Dual-layer distant phosphorus, described as two types of compounds with two correlated color temperatures (CCTs): 5,000 K and 8,500 K, are to be elucidated. Figure 1 depicts a WLED light with a protective-coating phosphor layer and an average CCT of 8,500 K in detail, note that the $C_7P_2S_2:Eu^{2+}$ phosphor is not included. The reflector's dimension is 8×9.85×2.07 mm for the length of bottom and top areas, and the height, respectively. The conformal phosphor compounding is used on nine 0.08 mm thick chips. A square base area of 1.14 mm^2 and a highness of 0.15 mm link every LED chip to the reflecting cavity. Every blue chip has a radiative flux of 1.16 W with a maximum wavelength of 453 nm.
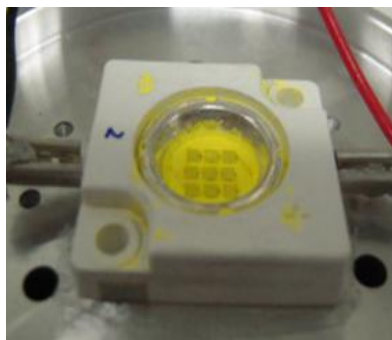

Figure 1. Photograph of WLEDs

3.   RESULTS AND ANALYSIS

Figure 2 reveals reversal changes in the concentrations of green $C_7P_2S_2:Eu^{2+}$ and yellow $YAG:Ce^{3+}$ phosphors. Figures 2(a) and 2(b) exhibits the changes under two CCT values of 5,000 K and 8,500 K, respectively. This opposite tendency has a function of keeping the consistency of the average CCTs. Moreover, this shows significant effects on the absorptivity and diffusing of WLEDs with two phosphor films, and consequently has certain impacts on the hue standard and WLEDs luminous flux performance. As a result, the color quality of WLEDs is determined by the chosen $C_7P_2S_2:Eu^{2+}$ concentration. When the $C_7P_2S_2:Eu^{2+}$ amount increased from 5% to 15% Wt., the $YAG:Ce^{3+}$ weight percentage declined to maintain the average CCTs. This can be observed in the cases of WLEDs with both preset CCTs of 5,000 K and 8,500 K.

Figure 3 depicts the influence of the $C_7P_2S_2:Eu^{2+}$ concentration on the transmitting spectrum of WLEDs. The correlation takes place under CCT values of 5,000 K and 8,500 K, exhibited via Figures 3(a) and 3(b), respectively. It is feasible to make a selection relying on the specifications provided by the producer. WLEDs that demand good hue fidelity can diminish luminous flux by a tiny amount. As shown in Figure 3, white light is the spectral region's synthesis. The spectra of 5,000 K and 8,500 K are shown in this diagram. Obviously, the strength trend grows with concentration $C_7P_2S_2:Eu^{2+}$ in two sections of the light spectrum: 420-480 nm and 500-640 nm. This rise in the output luminous flux may be seen in the two-band emission spectrum. When the blue-light scattering in WLEDs increases, imply that diffusing in the phosphorous film and WLEDs will increase as well, favoring color uniformity. When using $C_7P_2S_2:Eu^{2+}$, this is a significant outcome. Controlling the hue uniformity of the elevated heat distant phosphor configuration in particular is difficult. This article found that $C_7P_2S_2:Eu^{2+}$, at poor and elevated color temperatures (5,600 K and 8,500 K), provides high probability of achieving color-quality enhancement for WLEDs.
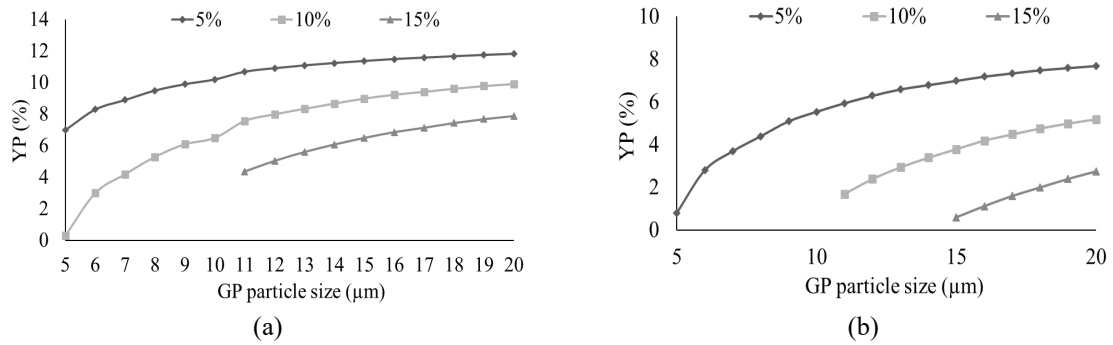
(a)

(b)

Figure 2. Shifting the phosphor concentration to keep the mean CCTs of (a) 5,000 K and (b) 8,500 K
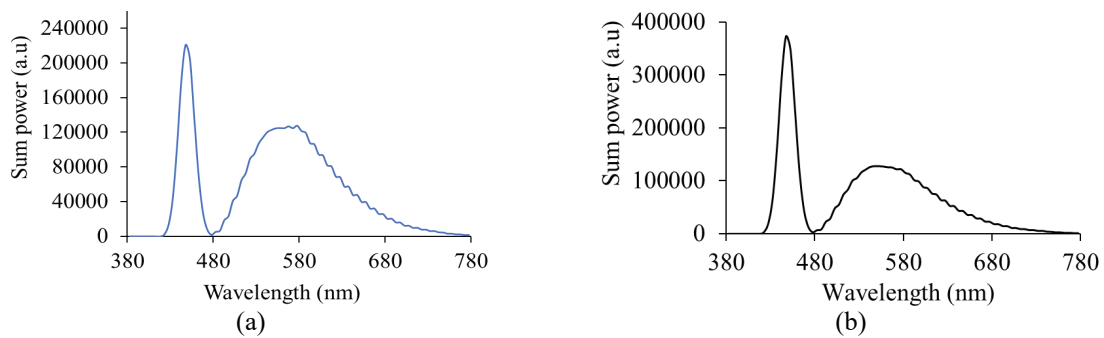

(a)

(b)

Figure 3. Emitting spectra of WLEDs as a function of $C_7P_2S_2:Eu^{2+}$ concentration under CCT values of
(a) 5,000 K and (b) 8,500 K

The efficiency of the emitted light flux of the simulated dual-film distant phosphor configuration was shown in the paper. The results in Figure 4 show that as the concentration of $Ca_7(PO_4)_2(SiO_4)_2:Eu^{2+}$ increased from 5% wt to 15% wt, the luminous flux emitted jumped dramatically up to around 175 lm, under both CCT values of 5,000 K and 8,500 K in Figures 4(a) and (b) respectively.
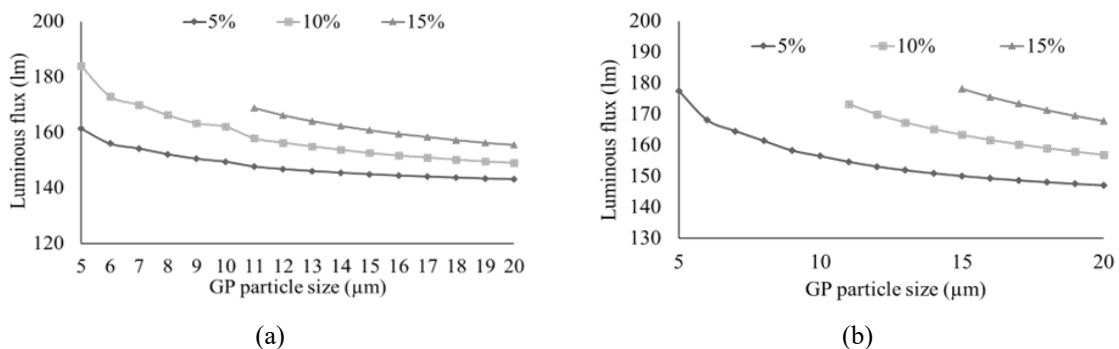

(a)

(b)

Figure 4. The luminous flux of WLEDs as a function of $C_7P_2S_2:Eu^{2+}$ concentration at CCT values of
(a) 5,000 K and (b) 8,500 K

Judging Figure 5, the color divergence was substantially reduced with the phosphor $Ca_7(PO_4)_2(SiO_4)_2:Eu^{2+}$ concentration, which can be observed in Figures 5(a), and (b), exhibiting CCT values of 5,000 K and 8,500 K, respectively. The reduction in chromatic variants is possibly attributed to the absorption efficiency of the green $C_7P_2S_2:Eu^{2+}$ phosphor compound. Particularly, the blue lights from the LED chip, when going through the yellow phosphor layer and reaching the $C_7P_2S_2:Eu^{2+}$ green phosphor, are

absorbed by the green phosphor particles. Then, these particles re-emits those light with green color. In other words, $C_7P_2S_2:Eu^{2+}$ layer significantly enhances the green spectral energy for the white lights via the effective blue-light absorption and conversion. $C_7P_2S_2:Eu^{2+}$ additionally absorbs the yellow light but in a much smaller amount, compared to the blue ones. As a result of the $C_7P_2S_2:Eu^{2+}$ addition, green-light contents in the WLED increase, improving the color uniformity index. Hue uniformity is one of the most necessary factors among current WLED light parameters. The more excellent the hue uniformity of the emitted white illumination presents, the more expensive the WLED is. However, the low cost of $C_7P_2S_2:Eu^{2+}$ is an advantage, which helps this phosphor material can be used in a variety of applications.
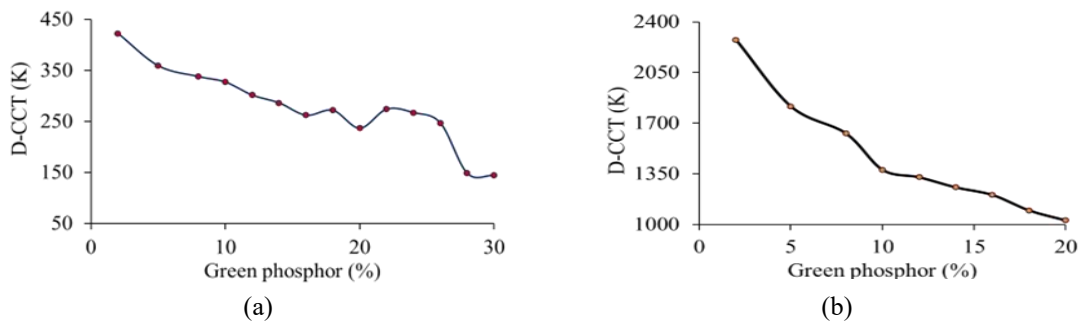

Figure 5. The hue deviation of WLEDs as a function of $C_7P_2S_2:Eu^{2+}$ concentration under CCT values of (a) 5,000 K and (b) 8,500 K

Color uniformity is only one criterion to consider when assessing WLED color quality. With just only an elevated hue homogeneity index, hue quality may not be stated to be good. As a result, current research has resulted in the development of a hue rendering index, abbreviated as CRI, and a hue standard scale, abbreviated as CQS. When light shines on the hue rendering index, it identify the hue accuracy of the light source on an object. The considerable abundance of green light, over the other key color elements of yellow and blue, apparently causes the color imbalance. This has an effect on the color quality of WLEDs, resulting in a decrease in color fidelity. The outcomes in Figure 6 show a small decline in CRI with the increase of $C_7P_2S_2:Eu^{2+}$ concentration in the distant phosphor package at 5,000 K and 8,500 K CCTs in Figures 6(a) and (b), respectively. Nonetheless, because CRI is simply a flaw in CQS, this decrease might be allowed. When comparing CRI with CQS, the CQS is more essential and harder to attain. CQS is a three-element index, with the first being the hue rendering index, the second being the viewer's preference, and the last being the hue coordinate. Among the three necessary factors, CQS is nearly a genuine overall assessment of hue quality. Figure 7 displays the increase of CQS in the presence of the remote phosphor $C_7P_2S_2:Eu^{2+}$ film under 5,000-K CCT in Figure 7(a) and 8,500 K CCT in Figure 7(b). Furthermore, when the $C_7P_2S_2:Eu^{2+}$ amount is raised, CQS does not change considerably as long as $C_7P_2S_2:Eu^{2+}$ concentration is under 10% wt. Both CRI and CQS are highly diminished when $C_7P_2S_2:Eu^{2+}$ concentrations are larger than 10% wt owing to severe hue loss when green-color is dominant. As a result, when utilizing green phosphor $C_7P_2S_2:Eu^{2+}$, proper concentration selection is critical.
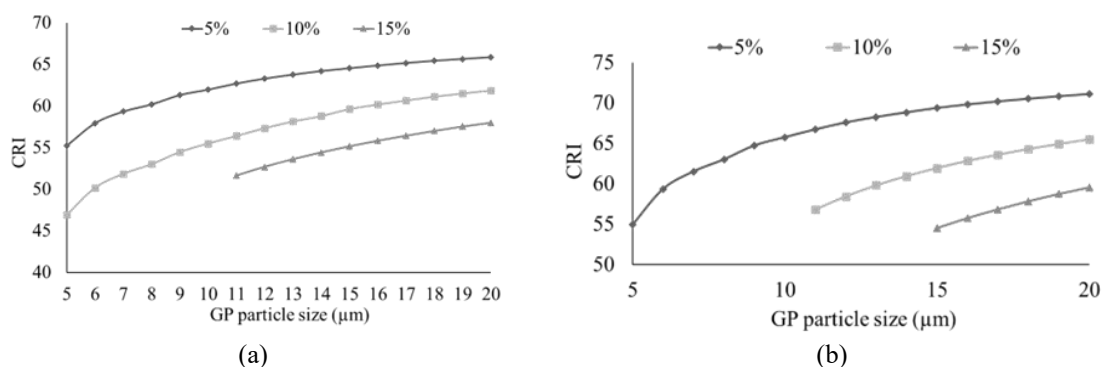

Figure 6. The hue rendering index of WLEDs as a function of $C_7P_2S_2:Eu^{2+}$ concentration under CCT values of (a) 5,000 K and (b) 8,500 K
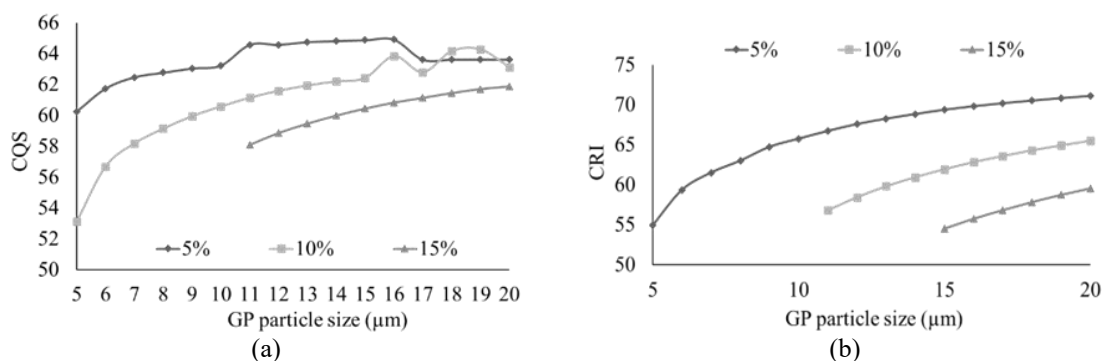
Figure 7. The hue quality scale of WLEDs as a function of $C_7P_2S_2$:Eu^{2+} concentration under CCT values of (a) 5,000 K and (b) 8,500 K

4. CONCLUSION

The effect of $Ca_7(PO_4)_2(SiO_4)_2$:Eu^{2+}, shortened form: $C_7P_2S_2$:Eu^{2+}, green phosphorus on the lighting efficiency of a double-layer phosphorus arrangement is discussed in this work. The study found that $C_7P_2S_2$:Eu^{2+} is a good selection help enhancing hue uniformity based on Monte Carlo computer simulations. It is true for WLEDs having the hue temperature of either 5,000 K or 8,500 K. The outcomes of this research have so achieved the goal of improving the chromaticity adequacy and luminous flux, which is difficult to do due to the remote configuration of phosphorus. CRI and CQS, on the other hand, have a tiny drawback. The CRI and CQS fall dramatically when the $Ca_7(PO_4)_2(SiO_4)_2$:Eu^{2+} concentration is increased excessively. As a result, the right concentration must be chosen based on the manufacturer's aims. The article has provided a large amount of useful data for generating higher hue uniformity and illuminating beam WLEDs.

ACKNOWLEDGEMENTS

REFERENCES
[1] R. Guerreiro, I. Carpinteiro, L. Proença, M. Polido, and A. Azul, "Influence of acid etching on internal bleaching with 16% carbamide peroxide," *Ann. Med.*, vol. 53, no. sup1, pp. S48--S49, Apr. 2021, doi: 10.1080/07853890.2021.1897351.
[2] A. Vagge, L. F. Desideri, C. D. Noce, I. D. Mola, D. Sindaco, and C. E. Traverso, "Blue light filtering ophthalmic lenses: A systematic review," *Semin. Ophthalmol.*, vol. 36, no. 7, pp. 541–548, Oct. 2021, doi: 10.1080/08820538.2021.1900283.
[3] S. Kadyan, S. Singh, S. Sheoran, A. Samantilleke, B. Mari, and D. Singh, "Synthesis and optoelectronic characteristics of MGdAl₃O₇:Eu³⁺ nanophosphors for current display devices," *Trans. Indian Ceram. Soc.*, pp. 219–226, Dec. 2019, doi: 10.1080/0371750X.2019.1690583.
[4] S. Sheoran *et al.*, "Synthesis and optoelectronic characterization of silicate lattice-based M₃La₂Si₃O₁₂ (M=Mg²⁺, Ca²⁺, Sr²⁺ and Ba²⁺) nanophosphors for display applications," *Trans. Indian Ceram. Soc.*, vol. 79, no. 1, pp. 35–42, Jan. 2020, doi: 10.1080/0371750X.2020.1712259.
[5] E. Bowditch, E. Chu, T. Hong, and A. A. Chang, "Treat and extend paradigm in management of neovascular age-related macular degeneration: current practice and future directions," *Expert Rev. Ophthalmol.*, vol. 16, no. 4, pp. 267–286, Jul. 2021, doi: 10.1080/17469899.2021.1933439.
[6] J. S. P. Antonio and P. Sanmartín, "Exposure to artificial daylight or UV irradiation (A, B or C) prior to chemical cleaning: an effective combination for removing phototrophs from granite," *Biofouling*, vol. 34, no. 8, pp. 851–869, Sep. 2018, doi: 10.1080/08927014.2018.1512103.
[7] L. M. Negi, S. Talegaonkar, M. Jaggi, and A. K. Verma, "Hyaluronated imatinib liposomes with hybrid approach to target CD44 and P-gp overexpressing MDR cancer: an in-vitro, in-vivo and mechanistic investigation," *J. Drug Target.*, vol. 27, no. 2, pp. 183–192, Feb. 2019, doi: 10.1080/1061186X.2018.1497039.
[8] M. Alavi and M. Rai, "Recent advances in antibacterial applications of metal nanoparticles (MNPs) and metal nanocomposites (MNCs) against multidrug-resistant (MDR) bacteria," *Expert Rev. Anti. Infect. Ther.*, vol. 17, no. 6, pp. 419–428, Jun. 2019, doi: 10.1080/14787210.2019.1614914.
[9] A. C. F. Vendette, H. L. Piva, L. A. Muehlmann, D. A. de Souza, A. C. Tedesco, and R. B. Azevedo, "Clinical treatment of intra-epithelia cervical neoplasia with photodynamic therapy," *Int. J. Hyperth.*, vol. 37, no. 3, pp. 50–58, Dec. 2020, doi: 10.1080/02656736.2020.1804077.
[10] M. Talone and G. Zibordi, "Spatial uniformity of the spectral radiance by white LED-based flat-fields," *OSA Contin.*, vol. 3, no. 9, p. 2501, Sep. 2020, doi: 10.1364/OSAC.394805.
[11] V. B. Yekta and T. Tiedje, "Limiting efficiency of indoor silicon photovoltaic devices," *Opt. Express*, vol. 26, no. 22, p. 28238, Oct. 2018, doi: 10.1364/OE.26.028238.
[12] B. Li *et al.*, "High-efficiency cubic-phased blue-emitting Ba₃ Lu₂ B₆ O₁₅ :Ce³⁺ phosphors for ultraviolet-excited white-light-emitting diodes," *Opt. Lett.*, vol. 43, no. 20, p. 5138, Oct. 2018, doi: 10.1364/OL.43.005138.

[13] S. Cincotta, C. He, A. Neild, and J. Armstrong, "High angular resolution visible light positioning using a quadrant photodiode angular diversity aperture receiver (QADA)," *Opt. Express*, vol. 26, no. 7, p. 9230, Apr. 2018, doi: 10.1364/OE.26.009230.
[14] Q. Hu, X. Jin, and Z. Xu, "Compensation of sampling frequency offset with digital interpolation for OFDM-Based visible light communication systems," *J. Light. Technol.*, vol. 36, no. 23, pp. 5488–5497, Dec. 2018, doi: 10.1109/JLT.2018.2876042.
[15] A. I. Alhassan *et al.*, "Development of high performance green c-plane III-nitride light-emitting diodes," *Opt. Express*, vol. 26, no. 5, p. 5591, Mar. 2018, doi: 10.1364/OE.26.005591.
[16] J. Cheng *et al.*, "Luminescence and energy transfer properties of color-tunable $Sr_4 La(PO_4)_3$ O: Ce^{3+}, Tb^{3+}, Mn^{2+} phosphors for WLEDs," *Opt. Mater. Express*, vol. 8, no. 7, p. 1850, Jul. 2018, doi: 10.1364/OME.8.001850.
[17] J.-S. Li, Y. Tang, Z.-T. Li, L.-S. Rao, X.-R. Ding, and B.-H. Yu, "High efficiency solid–liquid hybrid-state quantum dot light-emitting diodes," *Photonics Res.*, vol. 6, no. 12, p. 1107, Dec. 2018, doi: 10.1364/PRJ.6.001107.
[18] Y. Peng *et al.*, "Flexible fabrication of a patterned red phosphor layer on a $YAG:Ce^{3+}$ phosphor-in-glass for high-power WLEDs," *Opt. Mater. Express*, vol. 8, no. 3, p. 605, Mar. 2018, doi: 10.1364/OME.8.000605.
[19] K. Werfli *et al.*, "Experimental demonstration of high-speed 4 × 4 Imaging multi-CAP MIMO visible light communications," *J. Light. Technol.*, vol. 36, no. 10, pp. 1944–1951, May 2018, doi: 10.1109/JLT.2018.2796503.
[20] W. Zhong, J. Liu, D. Hua, S. Guo, K. Yan, and C. Zhang, "White LED light source radar system for multi-wavelength remote sensing measurement of atmospheric aerosols," *Appl. Opt.*, vol. 58, no. 31, p. 8542, Nov. 2019, doi: 10.1364/AO.58.008542.
[21] S. Feng and J. Wu, "Color lensless in-line holographic microscope with sunlight illumination for weakly-scattered amplitude objects," *OSA Contin.*, vol. 2, no. 1, p. 9, Jan. 2019, doi: 10.1364/OSAC.2.000009.
[22] J. O. Kim, H. S. Jo, and U. C. Ryu, "Improving CRI and scotopic-to-photopic ratio simultaneously by spectral combinations of cct-tunable led lighting composed of multi-chip leds," *Curr. Opt. Photonics*, vol. 4, no. 3, pp. 247–252, 2020, doi: 10.3807/COPP.2020.4.3.247.
[23] Z. Zhao, H. Zhang, S. Liu, and X. Wang, "Effective freeform TIR lens designed for LEDs with high angular color uniformity," *Appl. Opt.*, vol. 57, no. 15, p. 4216, May 2018, doi: 10.1364/AO.57.004216.

BIOGRAPHIES OF AUTHORS

Van Liem Bui 🆔 🅖 SC Ⓟ received a Bachelor of Mathematical Analysis and master's in mathematical Optimization, Ho Chi Minh City University of Natural Sciences, Vietnam. Currently, He is a lecturer at the Faculty of Fundamental Science, Industrial University of Ho Chi Minh City, Vietnam. His research interests are mathematical physics. He can be contacted at email: buivanliem@iuh.edu.vn.

Phan Xuan Le 🆔 🅖 SC Ⓟ received a Ph.D. in Mechanical and Electrical Engineering from Kunming University of Science and Technology, Kunming City, Yunnan Province, China. Currently, he is a lecturer at the Faculty of Engineering, Van Lang University, Ho Chi Minh City, Vietnam. His research interests are optoelectronics (LED), power transmission and automation equipment. He can be contacted at email: le.px@vlu.edu.vn.